Geofísica Internacional 49 (3), 153-163 (2010)

Intraslab Mexican earthquakes of 27 April 2009 (Mw5.8) and 22 May 2009 (Mw5.6): a source and ground motion study

UNAM Seismology group
X. Pérez-Campos[1*], S. K. Singh[1], A. Iglesias[1], L. Alcántara[2], M. Ordaz[2] and D. Legrand[1]
with contributions (in alphabetical order) by L. A. Aguilar[2], D. Almora[2], M. Ambriz[2], M. Ayala[2], C. Cárdenas[1], G. Castro[2], J. L. Cruz[1], R. Delgado[2], J. Estrada[1], S. I. Franco-Sánchez[1], M. A. Macías[2], I. Molina[2], F. Navarro[1], C. Pérez[2], J. Pérez[1], A. Quezada[1], L. Quintanar[1], L. E. Rodríguez[1], A. L. Ruiz[2], H. Sandoval[2], M. Torres[2], C. Valdés-González[1], R. Vázquez[2], J. M. Velasco[2], J. Velázquez[2], and M. Velázquez[2]
[1]*Instituto de Geofísica, Universidad Nacional Autónoma de México, Mexico City, Mexico*
[2]*Instituto de Ingeniería, Universidad Nacional Autónoma de México, Mexico City, Mexico*

Received: December 3, 2009; accepted: June 4, 2010

Resumen

Dos tipos de sismos intraplaca en la placa de Cocos que subduce debajo de la placa Norte America ocurren en Guerrero, México, y áreas adyacentes: (A) inversos de gran echado y (B) de fallamiento normal. Los de tipo A se localizan a ~10-35 km de la costa, a una profundidad de ~35 km, y revelan compresión en la dirección del echado de la placa, probablemente causada por su desdoblamiento. Los de tipo B son ligeramente más profundos que los del tipo A cuando ocurren cerca de la costa, pero si ocurren más adentro del continente, donde la placa se vuelve horizontal, alcanzan profundidades de 40-50 km. Estos eventos revelan extensión en la placa subducida orientada en la dirección de su echado.

El análisis de los sismos del 27 de abril y del 22 de mayo de 2009 revela que se trata de eventos intraplaca en la placa de Cocos subducida del tipo A y B, respectivamente. Los espectros de fuente obtenidos a partir de datos locales y regionales dan una caída de esfuerzos de Brune, $\Delta\sigma$, de ~49 y 34 MPa, respectivamente, un poco mayores que la mediana de $\Delta\sigma$ de 30 MPa reportada previamente para sismos intraplaca mexicanos. Nuestras estimaciones de energía radiada, E_R, son 3.55×10^{13} J y 2.29×10^{13} J, lo que arroja un cociente E_R/M_0 de 5.63×10^{-5} y 6.54×10^{-5}, y un esfuerzo aparente, σ_a, de 3.9 MPa y 4.6 MPa, respectivamente (correspondientes al M_0 reportado en el catálogo Global de CMT), valores razonables para sismos intraplaca.

Las aceleraciones máximas del terreno (PGA), como una función de la distancia están en buen acuerdo con relaciones de atenuación previamente obtenidas para sismos intraplaca mexicanos. Los movimientos del terreno en el Valle de México generados por sismos intraplaca son más ricos en altas frecuencias en comparación con aquéllos de eventos interplaca, especialmente en la zona dura. Esto refleja tanto una naturaleza más energética de las fuentes intraplaca como una distancia más cercana a la fuente de muchos de estos sismos. Los resultados obtenidos en este estudio nos dan confianza en nuestro conocimiento de la naturaleza de las fuentes intraplaca y nuestra habilidad de estimar movimientos fuertes para eventos futuros.

Palabras clave: Sismos intraplaca, geometría de la placa, energía radiada, movimiento del terreno.

Abstract

Two types of intraslab earthquakes in the subducted Cocos plate occur below Guerrero, Mexico, and adjacent areas: (A) steeply-dipping thrust earthquakes, and (B) normal-faulting earthquakes. Type A events are located ~10-35 km from the coast at a depth of ~35 km and reveal down-dip compression in the slab, most probably a consequence of unbending of the slab. Type B earthquakes are only slightly deeper than type A events when they occur near the coast, but if they occur farther inland where the slab becomes horizontal, they reach a depth of 40-50 km. They reveal down-dip extension in the subducted slab.

Analysis of earthquakes of 27 April 2009 and 22 May 2009 reveals that they were intraslab events in the subducted Cocos plate of type A and B, respectively. The source spectra retrieved from local and regional data yield Brune stress drop, $\Delta\sigma$, of ~49 and 34 MPa, respectively, somewhat greater than the median $\Delta\sigma$ of 30 MPa previously reported for intraslab Mexican earthquakes. Our estimates of the radiated energy, E_R, are 3.55×10^{13} J and 2.29×10^{13} J, which gives E_R/M_0 of 5.63×10^{-5} and 6.54×10^{-5}, and apparent stress, σ_a, of 3.9 MPa and 4.6 MPa, respectively (corresponding to M_0 reported in Global CMT catalog), reasonable values for intraslab earthquakes.

Peak ground accelerations (PGA) as a function of distance are in fairly good agreement with previously-derived attenuation relations for Mexican intraslab earthquakes. Ground motions in the Valley of Mexico from intraslab earthquakes are enriched at high frequency as compared to those from interplate events, especially in the hill zone. This reflects both a more energetic nature of the intraslab sources and, relatively, closer location of many of these earthquakes. The results obtained in this study give us some confidence in our knowledge of the nature of intraslab sources and our ability to estimate ground motions from future events.

Key words: Intraplate earthquakes, slab geometry, radiated energy, ground motion.

Introduction

Study of intraslab earthquakes in the subducting Cocos plate below Mexico is important in understanding the dynamics of the subduction as well as in the seismic hazard estimation. The intraslab earthquakes are often normal-faulting events involving down-dip extension. Some of these earthquakes have caused great damage in the Mexican altiplano. The earthquake of 15 January 1931 (M 7.8, H = 40 km) caused destruction to the City of Oaxaca (Singh *et al.,* 1985); the earthquakes of 28 August 1973 (M_w 7.0; H = 82 km) and 24 October 1980 (M_w 7.0; H = 65 km) resulted in deaths and damage in the states of Veracruz, Puebla, and Oaxaca (Singh and Wyss, 1976; Lomnitz, 1982; Yamamoto *et al*., 1984; Nava *et al*., 1985). Tehuacán earthquake of 15 June 1999 (M_w 7.0, H = 60 km) caused damage in the State of Puebla, especially to colonial structures in and near the city of Puebla (Singh *et al*., 1999). The great earthquake of 19 June 1858, which caused severe damage to inland towns in the state of Michoacán, including its capital city of Morelia, and to Mexico City, may also have been an intraslab, normal-faulting event (Singh *et al*., 1996).

The epicenters of the earthquakes mentioned above were in the altiplano. However, normal-faulting, intraslab earthquakes also occur near the coast. Earthquakes of 11 January 1997 (M_w 7.1; H = 35 km) and 30 September 1999 (M_w 7.4, H = 40 km) are two such examples. The 1997 earthquake occurred near Caleta de Campos below the rupture area of the 19 September 1985 Michoacán earthquake (Santoyo *et al*., 2005). The 1999 earthquake was located near the coast of Oaxaca and caused damage to towns along the coast and between the coast and the City of Oaxaca (Singh *et al*., 2000).

The geometry of the subducted Cocos slab below Guerrero is somewhat unusual. Several studies based on seismicity and focal mechanisms confirm the subduction of Cocos plate below Guerrero at a shallow angle, reaching a depth of 25 km at a distance of 65 km from the trench. The plate begins to unbend at this distance and becomes horizontal at a distance of ~120 km at a depth of ~40 km (Suárez *et al*., 1990; Singh and Pardo, 1993; Pardo and Suárez, 1995; Pacheco and Singh, 2010). This is supported by recent observations on the geometry of the subducted Cocos plate imaged from receiver function analysis (Pérez-Campos *et al*., 2008). Pacheco and Singh (2010) report that the unbending of the slab results in steeply-dipping, thrust earthquakes at a depth of about 35 km. These intraslab events, whose focal mechanisms show down-dip compression, occur about 10 km inland from the coast. Atoyac earthquake of 13 April 2007 (M_w 5.9, H = 37.5 km) was this type of event (Singh *et al*., 2007). Thus, intraslab earthquakes below Guerrero are not only of normal-faulting, down-dip extensional type, but also of down-dip compressional type.

Preliminary location of the earthquakes of 27 April and 22 May 2009 and their focal mechanisms obtained from centroid moment tensor inversion suggest that these were intraslab earthquakes. Here, we undertake a more detailed source and ground-motion study of these earthquakes.

Source parameters

The earthquakes were well recorded at local and regional distances by broadband and accelerographic networks of Instituto de Geofisica, UNAM and accelerographic networks of Instituto de Ingenieria, UNAM. We use these data, augmenting them with a few recordings from stations operated by CENAPRED, to study the characteristics of the two sources and the ground motions.

Locations of the two earthquakes, computed from local and regional data, are listed in Table 1 and their epicenters are plotted in Fig 1a. The locations of the events in the section shown in Fig. 1b at once reveal that they were intraslab earthquakes.

(a) Regional moment tensor inversion

A regional moment tensor (RMT) inversion scheme has been implemented by the Mexican National Seismogical Service (SSN) which routinely and automatically estimates moment tensor of moderate and large Mexican earthquakes using broadband seismograms (http://laxdoru.igeofcu.unam.mx/cmt). Here we briefly summarize the procedure.

An e-mail report by the SSN triggers the automatic computation of RMT for $M \geq 5.0$ earthquakes. The system

Table 1

Source parameters of the earthquakes of 27 April 2009 and 22 May 2009.

Date	Lat., °N	Long., °W	H, km	M_0, N-m	M_w	strike ϕ, °	*dip* δ, °	*rake* λ, °	Source
27 April 2009	17.100	99.430	33.3	6.3×10^{17}	5.8	277	68	100	Global CMT[1]
	16.971	99.566	37.4	3.8×10^{17}	5.7	285	82	99	This study[2]
	-	-	-	7.8×10^{17}	5.9	-	-	-	This study[3]
	-	-	-	9.7×10^{17}	5.9	280	65	85	This study[4]
22 May 2009	18.240	98.290	60.5	3.5×10^{17}	5.6	289	35	-60	Global CMT[1]
	18.100	98.434	45.5	3.0×10^{17}	5.6	286	39	-62	This study[2]
	-	-	-	4.6×10^{17}	5.7	-	-	-	This study[3]

[1]Global CMT solution
[2]Location from local and regional *P* and *S* phases data, and M_0 and focal mechanism from regional moment tensor inversion
[3]M_0 from *S*-wave spectra of local recordings
[4]M_0 and focal mechanism from inversion of near-source displacement traces

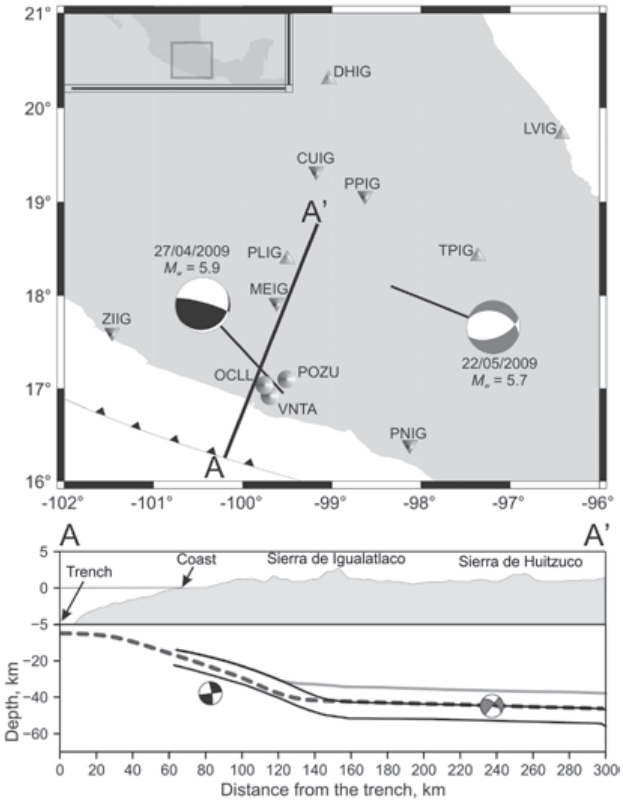

Fig. 1. (a) Tectonic setting of the Guerrero segment of the Mexican subduction. Seismicity and volcanism in the region is related to the subduction of Cocos plate below Mexico at a rate of ~6 cm/yr. Location and focal mechanism of the 27 April 2009 and 22 May 2009 earthquakes are marked. Broadband stations which were used in the regional moment tensor inversion are shown by inverted triangles (27 April event) and triangles (22 May event). Circles represent near-source accelerographic stations whose data for the 27 April earthquake were used to estimate focal mechanism and seismic moment (see text). (b) A section along AA', modified from Pacheco and Singh (2010). The plate interface inferred from seismicity (dashed line, Pacheco and Singh, 2010) and receiver functions (thin continuous line, Pérez-Campos *et al*., 2008) are indicated. Projections of the focal mechanisms for the 27 April, 2010 (dark) and 22 May, 2009 (light) earthquakes on AA' are shown.

chooses appropriate broadband stations according to magnitude reported as indicated in Table 2. Records from stations relatively close to the epicenter are discarded to avoid finite fault effects, and stations far from the epicenter are discarded to ensure good signal to noise ratio. Records of selected stations are integrated to obtain displacements and are band-pass filtered using frequencies that depend on magnitude (see Table 2). This procedure tries to use low frequencies (where displacement spectrum is flat), avoiding high frequencies at which the structure is poorly known. Selected seismograms are inverted using a time domain scheme implemented by Dreger (2003). Computation time is dramatically reduced using a set of stored Green's functions, which are computed at nodes of a grid of distances vs. depths and using an average *S*-wave velocity model. For Mexico, the SSN uses a model reported by Campillo *et al*. (1996).

Figures 2 and 3 illustrate the fit between observed and synthetic waveforms for the two earthquakes. These figures also provide a summary of the results. The focal mechanism of 27 April earthquake corresponds to steeply-dipping thrust faulting with downdip compression, while 22 May earthquake is a typical normal-faulting earthquake with downdip extension. The origin of 27 April earthquake may be interpreted as a consequence of unbending of the slab. Such unbending would give rise to compressional stress in the upper part of the subducted slab. The tensional stress corresponding to the 22 May earthquake may be attributed to negative buoyancy of the slab.

Table 2

Criteria for selection of BB stations and filters for RMT.

Magnitude (M_a or M_e)[1]	Distance intervals, km	Bandwidth, Hz
3.5 ≤ M < 5.0	30 < R < 400	0.02-0.05
5.0 ≤ M < 6.5	100 < R < 600	0.01-0.05
6.5 ≤ M < 7.5	200 < R < 995	0.01-0.05
7.5 ≤ M	500 < R < 995	0.05-0.02

[1]Singh and Pacheco (1994).

(b) Inversion of near-source recordings

We inverted near-source displacement records of the 27 April earthquake at POZU, VNTA, and OCLL (Fig. 1a), obtained by integration of the accelerograms, for focal mechanism and seismic moment. The inversion assumes that the events may be approximated by a point-source shear dislocation in an infinite space. Synthetic seismograms include near- and intermediate-field contributions (Singh *et al*., 2000). Theory predicts simple unipolar *P* and *S* displacement pulses. The effect of free surface is approximately taken into account by multiplying the infinite-space synthetics by two. This approximation is acceptable if the epicentral distance, Δ, is smaller than the depth, *H*. The fit between the observed and synthetic seismograms, shown in Fig. 4, is good. The focal mechanism and the moment are listed in Table 1. The source parameters obtained from near-source recordings and RMT inversion, and those reported in the Global Centroid Moment Tensor (CMT) catalog are reasonably similar.

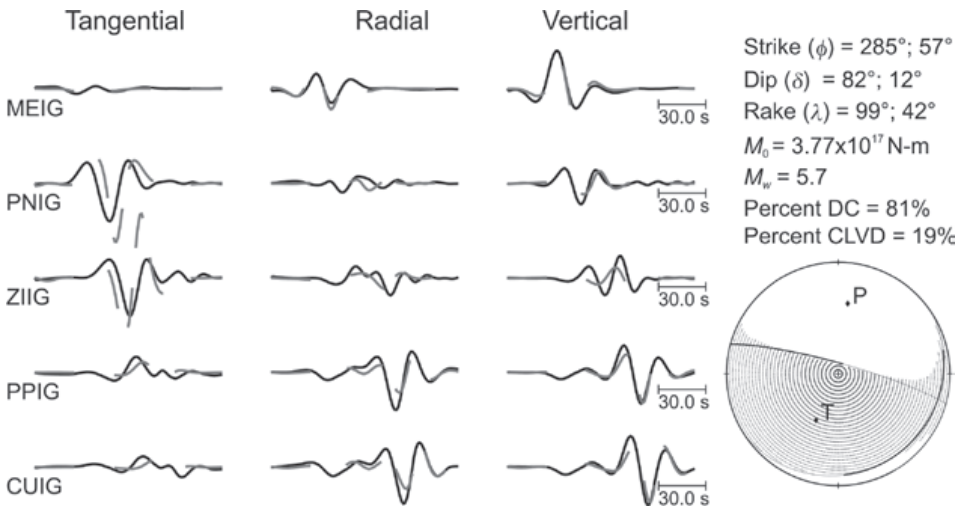

Fig. 2. Regional moment tensor inversion solution of the 27 April 2009 earthquake. Continuous and dashed lines represent observed and synthetic waveforms, respectively.

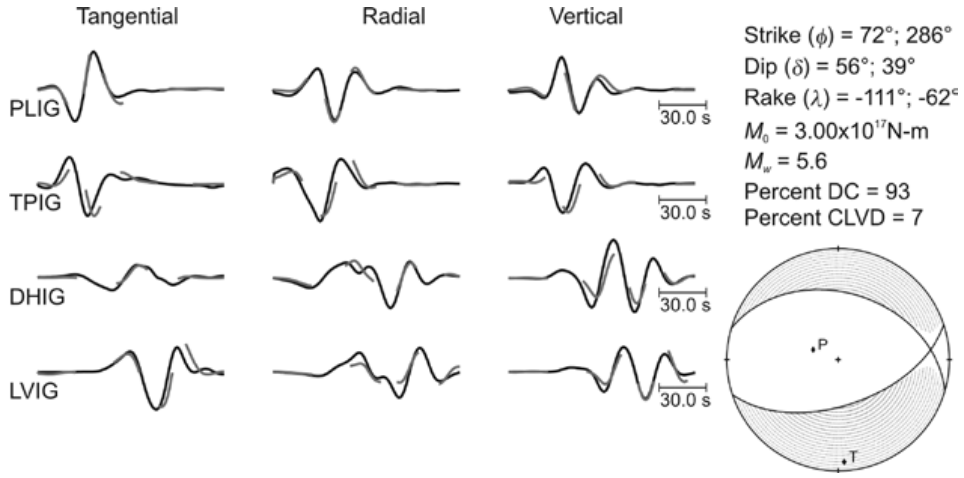

Fig. 3. Regional moment tensor inversion solution of the 22 May 2009 earthquake. Continuous and dashed lines represent observed and synthetic waveforms, respectively.

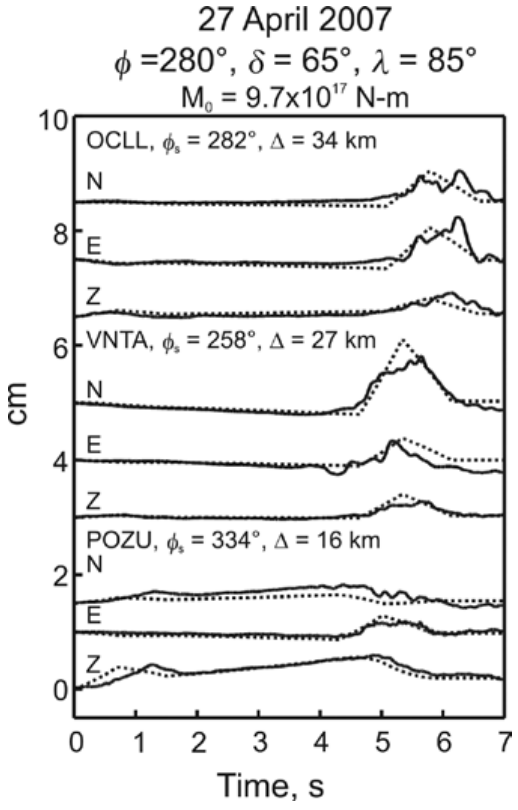

Fig. 4. Observed (continuous curves) and synthetic displacements (dashed curves) at stations POZU, VNTA, and OCLL (see Fig. 1a) during 27 April 2009 earthquake. Synthetic displacements correspond to the focal mechanisms and the seismic moments obtained from the inversion (see text).

The near-source displacement records of the 22 May earthquake are complex, and *P* and *S* pulses are not unipolar. For this reason, the simple inversion scheme, mentioned above, could not be used for this event.

(c) Source spectra

We estimated source displacement and acceleration spectra, $\dot{M}_0(f)$ and $f^2\dot{M}_0(f)$, of the two earthquakes from the analysis of the *S*-wave group recorded at hard sites. The Fourier acceleration spectral amplitude of the intense part of the ground motion at a station, under far-field, point-source approximation, may be written as

$$A(f, R) = Cf^2\,\dot{M}_0(f)G(R)e^{-\pi fR/\beta Q(f)}, \qquad (1)$$

where

$$C = FPR_{\theta\phi}(2\pi)^2 / (4\pi\rho\beta^3). \qquad (2)$$

In equations above, $\dot{M}_0(f)$ is the moment rate spectrum so that $\dot{M}_0(f)\rightarrow M_0$ as f→0, R = hypocentral distance, $R_{\theta\phi}$ = average radiation pattern (0.55), F = free surface amplification (2.0), P takes into account the partitioning of energy in the two horizontal components ($1/\sqrt{2}$), β = shear-wave velocity at the source, ρ = density in the focal region, and $Q(f)$ = quality factor which includes both anelastic absorption and scattering. The appropriate geometrical spreading term, $G(R)$, for inslab Mexican earthquakes is R^{-1} and the corresponding $Q(f)$ is $251f^{0.58}$ (García *et al*., 2004). As discussed in Pacheco and Singh (2010), the intraslab earthquakes below Guerrero occur in the lower oceanic crust or upper most part of the oceanic mantle. Assuming the source region of the earthquakes to

be in the upper mantle, we take $\beta = 4.68$ km/s and $\rho = 3.2$ kg/m^3. Taking logarithms of Equation (1) we obtain.

$$\log[A(f,R)]=\log C+\log[G(R)]+\log[f^2\dot{M}_0(f)]-1.36fR/\beta Q(f). \quad (3)$$

We solved Equation (3) in the least-squares sense to obtain $\log[f^2\dot{M}_0(f)]$.

The source displacement and acceleration spectra of the two earthquakes are shown in Figure 5. We interpret these spectra within the framework of a ω^2-source model and obtain an estimation of the seismic moment (M_0) and corner frequency (f_c). The stress drop ($\Delta\sigma$) is computed using the Brune model (Brune, 1970). The source spectra in Figure 5 can be fitted by M_0 and $\Delta\sigma$ of 7.8x10^{17} N-m and 49 MPa (f_c = 0.915 Hz), and 4.3x10^{17} N-m and 34 MPa (f_c = 0.99 Hz), respectively. We note that these stress drops are slightly greater than the median $\Delta\sigma$ of 30 MPa reported by García *et al*. (2004) for inslab Mexican earthquakes. The earthquake of 27 April 2009 is remarkably similar to the Atoyac earthquake of 13 April 2007 which was located ~90 km to the west and had about the same magnitude, depth, focal mechanism, and Brune stress drop (M_w 5.9; H = 37.5 km; $\phi = 284^0$, $\delta = 73^0$, $\lambda = 91^0$; $\Delta\sigma$ = 47 MPa; Singh *et al*., 2007) as the 2009 earthquake.

We emphasize that the source spectra and the estimated Brune stress drops above are contaminated by site effect. Although the sites are nominally "hard", weathering of near-surface rocks would give rise to amplification of seismic waves. These stress drops, however, are useful in estimating ground motions during future earthquakes using random vibration theory.

(d) Radiated seismic energy

Following Singh and Ordaz (1994), radiated seismic energy, E_R, can be written as:

$$E_R=\frac{4\pi R^2G^2(R)\rho\beta}{F^2R^2}2\int_0^\infty\left\{V_N^2(f)+V_E^2(f)+V_Z^2(f)\right\}\mathrm{A}(f)e^{2\pi fR/\beta Q(f)}df, \quad (4)$$

where $V_j(f)$ is the velocity spectrum of j-th component of the S-wave group. All other parameters are defined earlier. We used only hard-site recordings in the computation. Following Pérez-Campos *et al*. (2003), we applied a site effect correction that includes the combined effect of frequency-dependent site amplification and site attenuation (Boore, 1996; Boore and Joyner, 1997),

$$A(f) = A_0(f)e^{-\pi\kappa f}, \quad (5)$$

where $A_0(f)$ is the amplification factor, and was estimated from the generic rock model given by Boore and Joyner (1997), and κ is the attenuation parameter. Values of κ were obtained from Castro *et al*. (1990) and Humphrey and Anderson (1992), with an average value of $\kappa = 0.036$ s. E_R for the two events is plotted as a function of R in Fig. 6. The median E_R for the 27 April earthquake is 3.55x10^{13} J with 67% of observations lying within a factor of 2.7 of this value. For the 22 May earthquake the median E_R is 2.29x10^{13} J with 67% of observations lying within a factor of 2.3 of this value. This yields E_R/M_0 of 5.63x10^{-5} and 6.54x10^{-5} (corresponding to M_0 reported in Global CMT catalog) for the earthquakes of 27 April and 22 May, respectively.

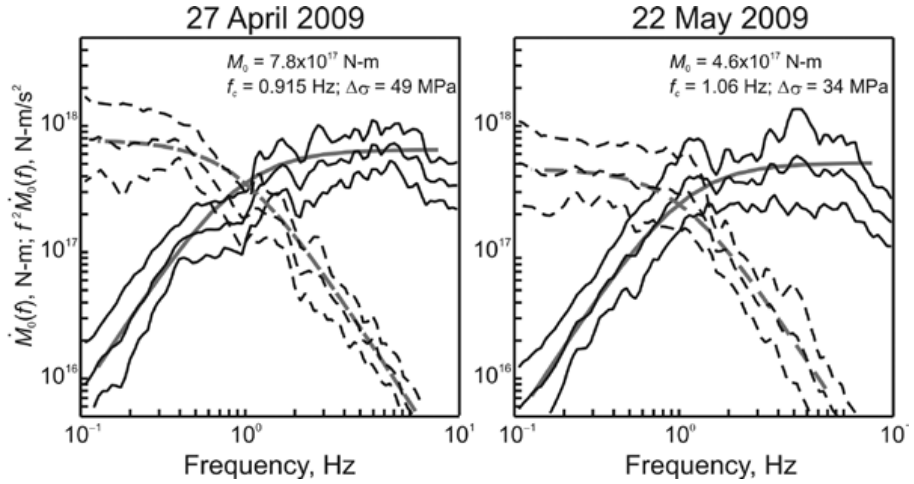

Fig. 5. Average source displacement (dasehd lines), $\dot{M}_0(f)$, and acceleration (solid lines), $f^2\dot{M}_0(f)$, spectra (mean and ±1 standard deviation curves). (Left) Earthquake of 27 April 2009 and (right) earthquake of 22 May 2009. Superimposed on the spectra are predicted curves from an ω^2 source model (smooth gray curves).

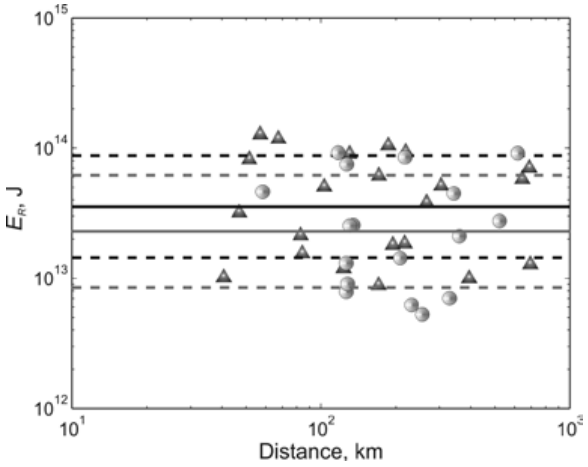

Fig. 6. Radiated seismic energy as function of distance for the 27 April 2009 (dark triangles), and 22 May 2009 (gray circles) earthquakes. The solid lines represent the mean value and the discontinued lines the mean plus/minus one standard deviation.

With $\mu = 7.0 \times 10^4$ MPa, the apparent stress, $\sigma_a = \mu E_R / M_0$, for the two earthquakes is 3.9 MPa and 4.6 MPa, respectively. These values of σ_a are similar to those found by Choy and Kirby (2004) for normal-faulting subduction earthquakes from a worldwide database. These authors report that the highest σ_a for inslab events occurred at 35-70 km depth, in proximity to zones of intense deformation such as sharp bends in the slab. The apparent stresses of these events were up to 5 MPa, significantly higher than for the interplate thrust earthquakes. Inslab earthquakes in Mexico are also significantly more energetic than interplate events (García *et al*., 2004).

For a Brune ω^2-source model, it can be shown that $\sigma_a = \mu E_R / M_0 = 0.23 \Delta\sigma$, where $\Delta\sigma$ is the Brune stress drop (see e.g., Singh and Ordaz, 1994). From $\Delta\sigma$ reported above, the expected σ_a for the two earthquakes are 11.3 MPa and 7.8 MPa, respectively, 2.9 and 1.7 times greater than the computed σ_a. The discrepancy, in part, arises from ignoring site effect in the estimation of $\Delta\sigma$.

Ground motions

(a) Peak Ground Acceleration (PGA) as a function of distance

Inasmuch as the Brune stress drops of the two earthquakes are about the same as the median stress drop of Mexican intraslab earthquakes, we expect the observed PGA to follow the attenuation relation obtained by García *et al*. (2005) for this type of earthquakes. The plot of PGA *versus* hypocentral distance *R* is shown in Fig. 7. In general, the observed PGA values follow the attenuation relation but there are some differences. For example, PGA for the vertical component of the 22 May earthquake is consistently lower than the expected values, especially for the broadband stations farther from the epicenter. This observation is also true for the horizontal component. For the 27 April event, the PGA values at close distances are consistently higher than those expected from García *et al*. (2005), no matter the type of site. There are some soft sites at ~300 km that show larger values of PGA than those expected. These correspond to sites within Mexico City.

In spite of the differences pointed out above, Fig. 7 gives us confidence in our ability to predict ground motion

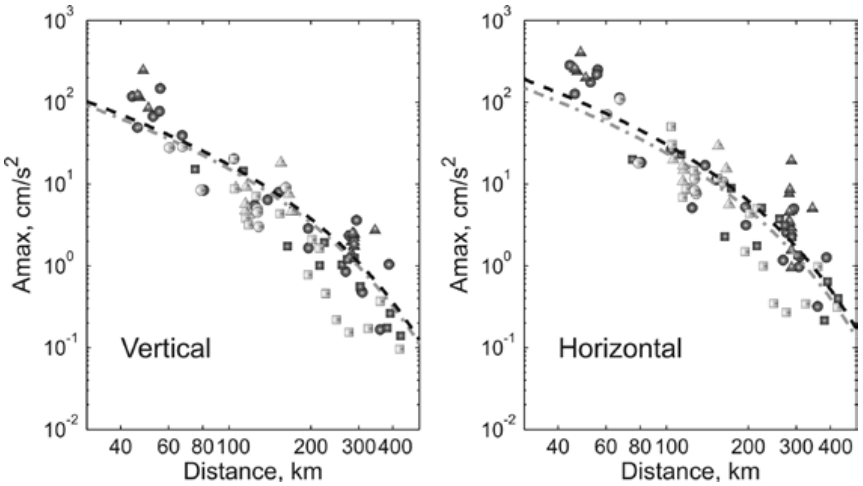

Fig. 7. PGA vs hypocentral distance for 27 April 2009 (dark) and 22 May 2009 (gray) earthquakes for the vertical (left) and horizontal (right) components. Triangles: soft strong motion sites; circles: hard strong motion sites; squares: hard broadband sites. The lines denote the expected relation between PGA and distance reported by García *et al*. (2005), using magnitude reported in Global CMT catalog; therefore each line represents the difference in both magnitude and depth between earthquakes.

from future intraslab earthquakes using the available attenuation relations.

(a) Ground motion in the Valley of Mexico: interplate versus intraslab earthquakes

Felt reports of intraslab earthquakes in the Valley of Mexico differ from those of interplate earthquakes. For events of the same magnitude, the ground motion from the former type of earthquakes felt more intense than from the latter type. This may be due to: (1) Location of intraslab events which, often, occur closer to the valley than the interplate events. The closest, well-located such earthquake has a hypocentral distance of 145 km (Iglesias *et al*., 2002), whereas interplate earthquake can only occur at $R > 250$ km. For the 22 May 2009 earthquake R to the city is ~160 km. (2) Depth of the intraslab earthquakes, which occur in the lower oceanic crust or the upper most mantle of the subducted slab, may give rise to significantly different wavefield in the valley than the interplate earthquakes. This is supported by theoretical computations (Furumura and Singh, 2002). García *et al*. (2004) show that intraslab earthquakes in Mexico are significantly more energetic than interplate events.

To illustrate the difference in the wavefield recorded in the valley, we compare ground motions from the interplate earthquake of San Marcos of 25 April 1989 (M_w 6.9; 16.6 °N, 99.5 °W; $H = 16$ km) and intraslab Tehuacán earthquake of 15 June 1999 (M_w 7.0; 18.15 °N, 97.52 °W, $H = 60$ km). Hypocentral distance of station CU (see Fig. 1), a hill-zone site, from the two events is 304 km and 225 km, respectively. Fig. 8 shows NS accelerograms recorded at CU, and at station SCT, a lake-bed site within the valley. We note that CU record of intraslab earthquake of Tehuacán is enriched at higher frequencies as compared to interplate earthquake of San Marcos. This difference is not visible at SCT. The Fourier spectra are illustrated in Fig. 9. For $f < 0.2$ Hz, the spectral amplitudes at CU and SCT are about the same. For $f > 0.2$ Hz, however, the amplitude spectra differ due to amplification of seismic waves at the lake-bed site of SCT (Figs. 9a and b). Comparison of spectra of the two earthquakes at CU (Fig. 9c) shows higher amplitudes at $f > 1$ Hz during the intraslab event of 1999 as compared to the interplate earthquake of 1989. The converse is true for $f < 1$ Hz. The spectra of the two earthquakes at SCT follow the same behavior as at CU, although higher amplitudes at SCT for $f > 1$ Hz during the intraslab earthquake is much less pronounced (Fig. 9d).

The larger spectral amplitudes in the hill zone at high frequencies ($f > 1$ Hz) during intraslab earthquakes may explain why the ground motion in this zone is felt more intensely during intraslab earthquakes as compared to interplate events. As shown in earlier studies (Singh *et al*., 1996; Iglesias *et al*., 2002), the relatively enriched high-frequency radiation in the hill zone renders small buildings in this zone vulnerable to strong intraslab earthquakes.

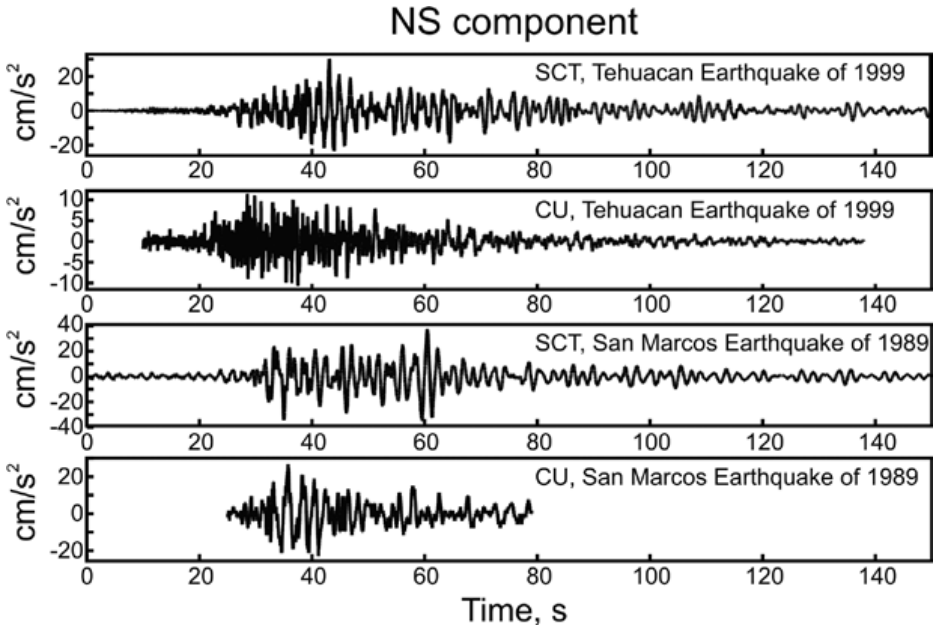

Fig. 8. NS component of acceleration at CU (hill-zone site) and SCT (lake-bed site) during interplate earthquake of San Marcos of 1989 (M_w 6.9) and intraslab earthquake of Tehuacán of 1999 (M_w 7.0). Note that CU recording during the Tehuacán earthquake is enriched at high frequencies as compared to the San Marcos earthquake.

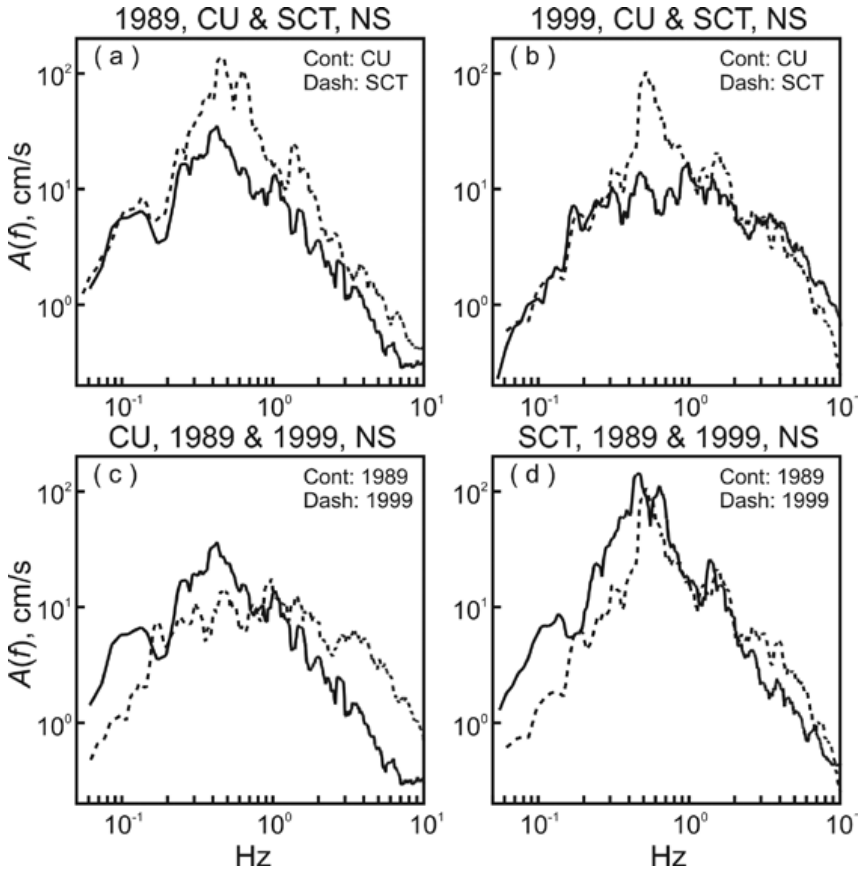

Fig. 9. Fourier spectra of NS component of acceleration at CU and SCT during San Marcos (1989) and Tehuacán (1999) earthquakes.

Discussion and conclusions

The intraplate earthquakes of 27 April and 22 May 2009 are examples of the two types of events that occur in the subducted slab below Guerrero: (A) steeply-dipping thrust events with down-dip compression and (B) normal-faulting earthquakes with down-dip tension. The former type seems to occur over a small distance range of ~15 to 40 km, inland from the coast, at a depth of about 35 km. Type (B) is observed over a larger distance range, ~15 to 175 km inland from the coast. The depth of this type of events is also ~35 km near the coast but increases to 40-50 km in the part of the slab where is horizontal. Thus, near the coast the two types of earthquakes occur in close proximity of each other. Within the uncertainty of the location, it is quite possible that type (B) occurs immediately below the type (A). Unbending of the slab provides an explanation for the occurrence of type (A) earthquakes, while negative buoyancy of slab may be the cause of the extensional stress observed over the longer distance range.

Intraslab earthquakes are more energetic at high frequencies than interplate events. However, there seems no discernible difference between the two types of intraslab events below Guerrero: the source spectra of both types can be explained by a stress drop of 30 to 50 MPa. The normalized energy, E_R/M_0, and apparent stress of the two earthquakes are ~6×10^{-4} and 4 MPa, respectively. These values are similar to those reported by Choy and Kirby (2004) for world-wide data base of normal-faulting intraslab earthquakes.

Observed PGA values of the two earthquakes are reasonably well fitted by a previously obtained attenuation relation (García *et al*., 2005). More energetic nature of the intraslab sources and their, often, closer location to the Valley of Mexico, produces ground motions in the hill-zone which are enriched in high frequencies. This may be the reason why felt reports of intraslab events suggest, relatively, intense motions. As shown in some previous studies (Singh *et al*., 1996; Iglesias *et al*., 2002), this is also the reason why smaller buildings in the hill zone may be vulnerable during large intraslab earthquakes.

Finally, the results of the analysis of the two earthquakes give us confidence in our knowledge of source characteristics of Mexican intraslab earthquakes and our ability to estimate ground motions from future such earthquakes.

Acknowledgements

The broadband network of SSN and the accelerographic network of II are partially funded by Secretaría de Gobernación, México. We thank CENAPRED for providing us with data from some of their stations. The research was partly supported by DGAPA (projects IN110207 and IN114809).

Bibliography

Boore, D. M., 1996. SMSIM-Fortran programs for simulating ground motions from earthquakes: version 1.0. U.S. Geol. Surv. *Open-File Rept. 96-80A, 96-80-B*, 69 pp.

Boore, D. M. and W. B. Joyner, 1997. Site amplifications for generic rock sites. *Bull. Seism. Soc. Am.*, *87*, 327-341.

Brune, J. N., 1970. Tectonic stress and the spectra of seismic shear waves from earthquakes. *J. Geophys. Res.*, *75*, 4997-5009.

Campillo, M., S. K. Singh, N. Shapiro, J. Pacheco and R. B. Hermann, 1996. Crustal structure of the Mexican volcanic belt, based on group velocity dispersion. *Geofísica Internacional*, *35*, *4*, 361-370.

Castro, R. R., J. G. Anderson and S. K. Singh, 1990. Site response, attenuation and source spectra of S waves along the Guerrero, Mexico subduction zone. *Bull. Seism. Soc. Am.*, *80*, 1481-1503.

Choy, G. L. and S. H. Kirby, 2004. Apparent stress, fault maturity and seismic hazard for normal-fault earthquakes at subduction zones. *Geophys. J. Int.*, *159*, 991-1012.

Dreger, D. S., 2003. TDMT_INV: Time Domain Seismic Moment Tensor INVersion. *International Handbook of Earthquake and Engineering Seismogy*, *81B*, 1627.

Furumura, T. and S. K. Singh, 2002. Regional wave propagation from Mexican subduction zone earthquakes: The attenuation functions for interplate and inslab events. *Bull. Seism. Soc. Am.*, *92*, 2110-2125.

García, D., S. K., Singh, M. Herráiz, M. Ordaz, and J. F. Pacheco, 2005. Inslab earthquakes of central Mexico: Peak ground-motion parameters and response spectra. *Bull. Seism. Soc. Am.*, *95*, 2272-2282.

García, D., S. K. Singh, M. Herráiz, J. F. Pacheco and M. Ordaz, 2004. Inslab earthquakes of central Mexico: Q, source spectra and stress drop. *Bull. Seism. Soc. Am.*, *94*, 789-802.

Humphrey, J. R. Jr. and J. G. Anderson, 1992. Shear-wave attenuation and site response in Guerrero, Mexico. *Bull. Seism. Soc. Am.*, *81*, 1622-1645.

Iglesias, A., S. K. Singh, J. F. Pacheco and M. Ordaz, 2002. A source and wave propagation study of the Copalillo, Mexico earthquake of 21 July, 2000 (M_w=5.9): Implications for seismic hazard in Mexico City from inslab earthquakes. *Bull. Seism. Soc. Am.*, *92*, 885-895.

Lomnitz, C., 1982. Direct evidence of a subducted plate under southern Mexico. *Nature*, *296,* 235-238.

Nava, F. A., V. Toledo and C. Lomnitz, 1985. Plate waves and the 1980 Huajuapan de Leon, Mexico earthquake. *Tectonophysics*, *112*, 463-492.

Pacheco, J. F. and S. K. Singh, 2010. Seismicity and state of stress in Guerrero segment of the Mexican subduction zone. *J. Geophys. Res.*, *115*, doi:10.1029/2009JB006453.

Pardo, M. and G. Suárez, 1995. Shape of the subducted Rivera and Cocos plates in southern Mexico: Seismic and tectonic implications. *J. Geophys. Res.*, *100*, 12, 357-12,373.

Pérez-Campos, X., Y. H. Kim, A. Husker, P. M. Davis, R.W. Clayton, A. Iglesias, J. F. Pacheco, S. K. Singh, V. C. Manea and M. Gurnis, 2008. Horizontal subduction and truncation of the Cocos plate beneath central Mexico. *Geophys. Res. Lett.*, *35*, L18303, doi: 10.1029/2008GL035127.

Pérez-Campos, X., S. K. Singh and G. C. Beroza, 2003. Reconciling teleseismic and regional estimates of seismic energy. *Bull. Seism. Soc. Am.*, *93,* 2123-2130.

Santoyo, M., S. K. Singh and T. Mikumo, 2005. Source process and stress change associated with the 11 January, 1997 (M_w=7.1) Michoacan, Mexico, inslab earthquake. *Geofísica Internacional*, *44*, 317-330.

Singh, S. K. and M. Ordaz, 1994. Seismic energy release in Mexican subduction zone earthquakes. *Bull. Seism. Soc. Am.*, *84*, 1533-1550.

Singh, S. K., M. Ordaz, L. Alcántara, N. Shapiro, V. Kostoglodov, J. F. Pacheco, S. Alcocer, C. Gutiérrez, R. Quaas, T. Mikumo, and E. Ovando, 2000. The Oaxaca Earthquake of September 30, 1999 (M_w=7.5): A Normal-Faulting Event in the Subducted Cocos Plate. *Seism. Res. Lett.*, *71*, 67-78.

Singh, S. K., M. Ordaz, J. F. Pacheco, L. Alcántara, A. Iglesias, S. Alcocer, D. García, X. Pérez-Campos, C. Valdes and D. Almora, 2007. A report on the Atoyac, Mexico, earthquake of 13 April 2007 (M 5.9). *Seism. Res. Lett.*, *78*, 635-648.

Singh, S. K., M. Ordaz, J. F. Pacheco and F. Courboulex, 2000. A simple source inversion scheme for displacement seismograms recorded at short distances. *J. Seism.*, *4*, 267-284.

Singh, S. K., M. Ordaz, J. F. Pacheco, R. Quaas, L. Alcántara, S. Alcocer, C. Gutiérrez, R. Meli and E. Ovando, 1999. A preliminary report on the Tehuacan, Mexico earthquake of June 15, 1999 (Mw=7.0). *Seism. Res. Lett.*, *70,* 489-504.

Singh, S. K., M. Ordaz and L. E. Pérez-Rocha, 1996. The great Mexican earthquake of 19 June 1858: Expected ground motions and damage in Mexico City from a similar future event. *Bull. Seism. Soc. Am.*, *86*, 1655-1666.

Singh, S. K. and J. Pacheco, 1994. Magnitude determination of Mexican earthquakes. *Geofísisca Internacional*, *33*, 189-198.

Singh, S. K. and M. Pardo, 1993. Geometry of the Benioff Zone and state of stress in the overriding plate in Central Mexico. *Geophys. Res. Lett.*, *20*, 1483-1486.

Singh, S. K., G. Suárez and T. Domínguez, 1985. The great Oaxaca earthquake of 15 January 1931: Lithosphere normal faulting in the subducted Cocos plate. *Nature*, *317*, 56-58.

Singh, S. K. and M. Wyss, 1976. Source parameters of the Orizaba earthquake of August 28, 1973. *Geofísica Internacional*, *16*, 165-184.

Suárez, G., T. Monfret, G. Wittlinger and C. David, 1990. Geometry of subduction and depth of the seismogenic zone in the Guerrero gap, Mexico. *Nature*, *345*, 336-338.

Yamamoto, J., Z. Jimenéz and R. Mota, 1984. El temblor de Huajuapan de Leon, Oaxaca, México, del 24 de Octubre de 1980. *Geofísica Internacional*, *23*, 83-110.

X. Pérez-Campos[1*], S. K. Singh[1], A. Iglesias[1], L. Alcántara[2], M. Ordaz[2] and D. Legrand[1]

[1]*Instituto de Geofísica, Universidad Nacional Autónoma de México, Ciudad Universitaria, Del. Coyoacán, 04510, Mexico City, Mexico*

[2]*Instituto de Ingeniería, Universidad Nacional Autónoma de México, Ciudad Universitaria, Del. Coyoacán, 04510, Mexico City, Mexico*

**Corresponding author: xyoli@geofisica.unam.mx*